Research Square

Preprints are preliminary reports that have not undergone peer review.
They should not be considered conclusive, used to inform clinical practice,
or referenced by the media as validated information.

Evolutionary Architecture of Longevity Regulators: Directional Conservation and Divergence from Yeast to Human Cells

Davis W. Cheng

dcheng@rockybiotech.org

Rocky Institute of Biotechnology

Research Article

Keywords: Lifespan, Cellular senescence, Comparative genetics, Yeast replicative lifespan, Autophagy, Antagonistic pleiotropy

Posted Date: November 13th, 2026

DOI: https://doi.org/10.21203/rs.3.rs-11543523/v1

License: This work is licensed under a Creative Commons Attribution 4.0 International License.
Read Full License

Additional Declarations: No competing interests reported.

Evolutionary Architecture of Longevity Regulators: Directional Conservation and Divergence from Yeast to Human Cells

Davis W. Cheng, Ph.D.

Rocky Institute of Biotechnology, Clovis, California, USA · ORCID 0009-0001-1306-8923

Correspondence: dcheng@rockybiotech.org

Running title: Evolutionary architecture of longevity regulators

Abstract

Targeted genetic perturbations in yeast, nematodes, fruit flies, mice and human cells have revealed thousands of regulators of lifespan and cellular senescence, and these regulators are shared across species more often than expected by chance. Whether the direction of their effects is conserved between experimental systems has not been examined systematically. We integrated 4,771 controlled genetic perturbations affecting yeast replicative lifespan (RLS) and chronological lifespan (CLS), nematode, fly and mouse lifespan, and human-cell senescence (3,399 human orthologs), classified each by direction of effect, and quantified directional conservation between systems. RLS and CLS shared regulators 1.7-fold more often than expected, yet their directions agreed only at chance (50%). RLS agreed with the direction of animal lifespan effects for 67% of genes ($P = 3 \times 10^{-6}$), whereas CLS agreed for 50%. When two or more non-mammalian organisms concurred, the mouse direction matched in 13 of 14 genes (93%), compared with 61% for single-organism evidence; this criterion nominates 180 untested genes. Human-cell senescence agreed with organismal lifespan for autophagy/proteostasis (82%) and mitochondrial/redox genes (73%), but only at chance for cell-cycle arrest and inflammatory-secretion genes (51–54%). Aging-restraining genes were more frequently essential for mouse development than aging-promoting genes (57% vs 48%; $P < 0.001$). Most of a 116-gene core shared by at least three systems formed a single network linking nutrient signaling with autophagy and redox maintenance. Longevity regulators are thus directionally conserved through yeast replicative lifespan, concordant non-mammalian evidence and maintenance functions, but diverge in senescence arrest and secretory pathways.

Keywords Lifespan · Cellular senescence · Comparative genetics · Yeast replicative lifespan · Autophagy · Antagonistic pleiotropy

1. Introduction

Loss- and gain-of-function studies in yeast, nematodes, fruit flies and mice have uncovered hundreds of genes that modulate lifespan (Kenyon et al. 1993; Hamilton et al. 2005; Hansen et al. 2005; McCormick et al. 2015), and perturbation studies in cultured human cells have defined a comparable number of regulators of cellular senescence (Hayflick and Moorhead 1961; Serrano et al. 1997; Coppé et al. 2008). These findings are curated in GenAge and CellAge (Tacutu et al. 2018; Avelar et al. 2020; de Magalhães et al. 2024). The same experimental logic, altering one gene against an otherwise constant genetic background, originally defined programmed cell death and autophagy as conserved cellular programs (Ellis and Horvitz 1986; Tsukada and Ohsumi 1993).

The sharing of aging-associated genes across species is well documented. Budovsky et al. (2007) mapped longevity genes from several model organisms to their human orthologs and showed that the encoded proteins form a connected interaction network. Smith et al. (2008) reported that 15% of yeast deletions targeting orthologs of nematode aging genes were long-lived, compared with 3.4% of random deletions. Yanai et al. (2017) analyzed 1,805 longevity-associated genes and found their orthologs overrepresented across taxa, with largely concordant effects among model organisms. Avelar et al. (2020) demonstrated that senescence-inducing genes overlap anti-longevity genes and that senescence genes are conserved in mammals but considerably less so in invertebrates.

These studies did not determine under which conditions the direction of an effect is preserved from one experimental system to another, which is the information required before a model-organism finding is pursued in mammals. Three issues remain unresolved. First, yeast offers two lifespan assays, replicative (RLS) and chronological (CLS), which are frequently pooled, and it is unknown which of them, if either, predicts the direction of effect in animals. Second, the degree of replication among non-mammalian organisms required to predict a mammalian outcome has not been quantified. Third, it is unknown which classes of human senescence regulators exert organismal lifespan effects of the same sign. A further issue concerns evolutionary interpretation: antagonistic pleiotropy predicts that aging-promoting genes are preferentially required early in life, a prediction that can be evaluated only with direction-resolved data.

Here we integrate 4,771 controlled genetic perturbations spanning yeast RLS and CLS, nematode, fly and mouse lifespan, and human-cell senescence; harmonize their direction of effect; and map them to human orthologs by database identifier. After establishing cross-species convergence under explicit bias controls, we quantify directional conservation between the two yeast assays, between concordant non-mammalian evidence and mice, and between human-cell senescence and organismal lifespan within functional categories, and we evaluate the antagonistic-pleiotropy prediction against mouse developmental essentiality. Finally, we characterize the network formed by regulators shared by at least three systems.

2. Materials and Methods

2.1 Study rationale and data sources

Only experiments in which a single gene was changed against a defined genetic background, under standard laboratory conditions, were used. Population association studies, drug treatments and dietary interventions were excluded. Data were downloaded on 19 October 2026 and downloaded again on 22 October 2026 for the final analysis; the original pipeline gave identical results on both downloads. GenAge and CellAge are part of the Human Ageing Genomic Resources (de Magalhães et al. 2024). No new experiments were performed.

Table 1. Controlled genetic-perturbation datasets used in this study

System	Source	What was changed	What was measured	Genes with an effect	Aging-promoting / restraining / mixed	Human genes after ortholog mapping
Yeast replicative lifespan (RLS)	phenotype annotations (Engel et al. 2025)	Deletion, reduction or overexpression; 98% in the S288C background	Number of daughters a mother cell produces	1,043	611 / 412 / 20	895
Yeast chronological lifespan (CLS)	SGD	As above	Survival of non-dividing cells	1,638	518 / 985 / 135	1,360
Worm lifespan	model organisms, Build 21 (Tacutu et al. 2018)	Mutation or RNAi in laboratory strains	Lifespan	887	578 / 283 / 28	1,140
Fly lifespan	GenAge Build 21	Mutation, transgene or RNAi	Lifespan	201	73 / 125 / 4	286
Mouse lifespan	GenAge Build 21	Knockout or transgene in inbred strains	Lifespan	136	45 / 85 / 6	147
Human cell senescence	Build 3 (Avelar et al. 2020)	Knockdown, knockout or overexpression in cultured cells	Induction or inhibition of replicative, oncogene-induced or stress-induced senescence	866	370 / 475 / 21	866

Yeast entries were restricted to annotations without a chemical or dietary condition. Mutant type was taken from SGD; deletion alleles (Δ) and the systematic deletion collection were treated as null.

2.2 Harmonization of effect direction

Effects were harmonized according to the inferred contribution of normal gene activity to the measured aging-related endpoint. A gene was classified as aging-promoting (AP) when its reduction or deletion extended lifespan or suppressed senescence, or when overexpression shortened lifespan or induced

senescence. Aging-restraining (AR) denoted the converse relationships. GenAge anti-longevity and pro-longevity annotations were coded AP and AR, respectively; CellAge senescence-inducing and senescence-inhibiting annotations were coded AP and AR. Conflicting annotations were resolved by majority classification, with ties designated mixed. These operational labels do not imply that senescence induction and organismal lifespan shortening are biologically equivalent.

2.3 Orthology

Non-human genes were mapped to human genes with the Alliance of Genome Resources combined orthology file (Alliance of Genome Resources Consortium 2024; version 9.0.0, "stringent" filter), retaining pairs supported by at least three prediction methods and ranked best in at least one direction, and retaining only human protein-coding genes (NCBI Gene). Genes were matched by database identifier, not by symbol: yeast genes by SGD identifier, and worm, fly and mouse GenAge genes by their NCBI Entrez Gene identifier, converted to WormBase, FlyBase or MGI identifiers through the cross-references in the NCBI gene_info files. Identifier-based matching was required because many GenAge symbols predate current nomenclature (for example, fly Tor, Sir2 and Sod); matching by symbol would have omitted 42 of 202 fly and 88 of 889 worm entries. Six GenAge entries that tested a human transgene (human G6PD, GMFB, NUDT1 and SOD3 in mice; human OTC and UCP2 in flies) were assigned directly to that human gene. For each organism, a human gene took the majority direction of its mapped source genes. The analysis universe for each organism was the set of human genes with any ortholog in that organism (yeast 4,107; worm 8,964; fly 10,141; mouse 18,133).

2.4 Convergence across organisms

For each pair of organisms, overlap between their human-mapped aging gene sets was tested by one-sided Fisher's exact test within the shared ortholog universe. Among overlapping genes with a resolved directional annotation in both organisms, the proportion acting in the same direction was tested against 50% by one-sided binomial test; Benjamini–Hochberg q-values across the ten pairs are also reported. To determine whether genes supported by several organisms occur more often than expected, 1,000 random gene sets of the observed sizes were drawn within each organism's universe (seed 20261019), and the number of genes appearing in at least 2, 3, 4 or 5 organisms was compared with the observed number. Genes with effects in at least three organisms were defined as core genes. For these analyses, yeast replicative and chronological lifespan were pooled, with each human gene assigned the majority direction across all mapped yeast genes in both assays; the two assays were analyzed separately as described in Section 2.6.

2.5 Network and functional analysis

Core genes were submitted to STRING version 12.5 (Szklarczyk et al. 2025), keeping interactions with a combined score of at least 0.7. Interaction enrichment was taken from STRING, and modules were defined by Louvain community detection (Blondel et al. 2008; NetworkX; seed 1). Each gene was matched to the STRING protein with the identical symbol; MAPK10 has no such entry in STRING 12.5 (its symbol resolves to DUSP16) and was left out, so 115 genes entered the network. Module stability was assessed by repeating community detection with 100 random seeds (adjusted Rand index against seed 1). Functional enrichment used g:Profiler (Kolberg et al. 2023) for GO Biological Process, GO Cellular Component, KEGG and Reactome, with g:SCS correction, against two backgrounds: the whole genome and, more stringently, all 3,399 human genes with an aging effect in any organism.

2.6 Direction-transfer analyses

Directional conservation between two systems was defined as the proportion of genes with a resolved (aging-promoting or aging-restraining) direction in both systems that acted in the same direction, tested against 50% by two-sided binomial test. Three comparisons were performed.

Yeast assays. RLS and CLS directions were assigned separately at the human-ortholog level (majority across mapped yeast genes). Their overlap was tested by one-sided Fisher's exact test within the yeast ortholog universe, and their directions were compared with each other and, for each assay, with the animal consensus, defined as the majority of resolved nematode, fly and mouse directions (ties excluded). The RLS–CLS comparison was repeated at the level of yeast genes without ortholog mapping.

Cross-species replication. For genes with a resolved mouse direction, the mouse direction was compared with the non-mammalian direction in two groups: genes for which at least two of yeast, nematode and fly had resolved and mutually concordant directions, and genes for which exactly one of these organisms had a resolved direction. Genes with conflicting non-mammalian directions were excluded, and the two proportions were compared by Fisher's exact test. To account for one-to-many orthology, the analysis was repeated after collapsing human genes that map to an identical set of non-human source genes. Genes satisfying the replication criterion that possess a mouse ortholog but lack a mouse lifespan annotation were compiled as predictions (Supplementary Table S9). For human cells, CellAge directions were compared with the organismal consensus (majority of resolved yeast, nematode, fly and mouse directions), stratified according to whether that consensus rested on one or on at least two organisms; the two strata were compared by Fisher's exact test. In the replication and human-cell analyses, the yeast direction corresponds to the pooled RLS and CLS direction described in Section 2.4.

Functional categories. The comparison between human cells and organisms was repeated within each functional category (Section 2.7), with Benjamini–Hochberg q-values computed across the eight categories. Maintenance categories (autophagy and proteostasis; mitochondria and redox) were compared with arrest and inflammatory categories (cell-cycle arrest and checkpoints; senescence-associated secretory phenotype [SASP] and inflammation) by Fisher's exact test after excluding genes assigned to both groups.

2.7 Functional categories and ortholog conservation

Genes were assigned to eight functional categories using Gene Ontology annotations (Gene Ontology Consortium 2023; UniProt-GOA human file of 11 October 2026, excluding NOT annotations), propagated to all ancestor terms of go-basic (release 2026-07-26): growth and nutrient signaling (TOR, insulin and IGF receptor signaling); DNA damage, repair and telomeres; cell-cycle arrest and checkpoints; chromatin and epigenetic regulation; autophagy and proteostasis; mitochondria and redox; SASP and inflammation (inflammatory response, cytokine signaling and production); and cell-death regulation. A gene could belong to more than one category. For the human cell-senescence genes in each category we recorded two quantities: the share with a yeast ortholog (ortholog conservation) and the share whose ortholog also changes lifespan in yeast, worm, fly or mouse (organismal lifespan coverage).

2.8 Subcellular localization and developmental essentiality

Subcellular location came from the Human Protein Atlas subcellular atlas (Uhlén et al. 2015), using main and additional locations. Requirement for development came from Mouse Genome Informatics (Baldarelli et al. 2024): a gene was scored as developmentally essential if any single-gene mouse genotype showed embryonic, prenatal, perinatal, neonatal, preweaning or postnatal lethality. Human–mouse orthology was taken from MGI. Groups were compared by Fisher's exact test.

2.9 Bias checks

Two biases were addressed. First, genes chosen for study in one organism because of results in another inflate apparent convergence. We therefore repeated the yeast overlaps using only genome-wide, hypothesis-free yeast deletion screens. Second, well-studied genes are more likely both to have aging data and to have mouse knockouts with severe phenotypes. We therefore fitted logistic regressions of lethality on aging evidence with the number of phenotyped single-gene mouse genotypes (log10) as a covariate.

2.10 Software, reproducibility and use of AI tools

Analyses were performed in Python 3 (pandas, NumPy, SciPy, statsmodels, NetworkX, scikit-learn, Matplotlib). Under the author's direction, an AI model (Claude, Anthropic) was used to retrieve the public datasets, write and execute the analysis code, assign Gene Ontology annotations, generate the figures, and revise the manuscript text for its readability from the author's original manuscript. The author directed and reviewed the code and outputs, finalized the text, and takes full responsibility for the content. Scripts 12–22, intermediate tables and figure files are provided as Supplementary Information; the directional-conservation analyses and Fig. 3 are generated by scripts 21 and 22.

3. Results

3.1 A harmonized catalog of controlled genetic perturbations

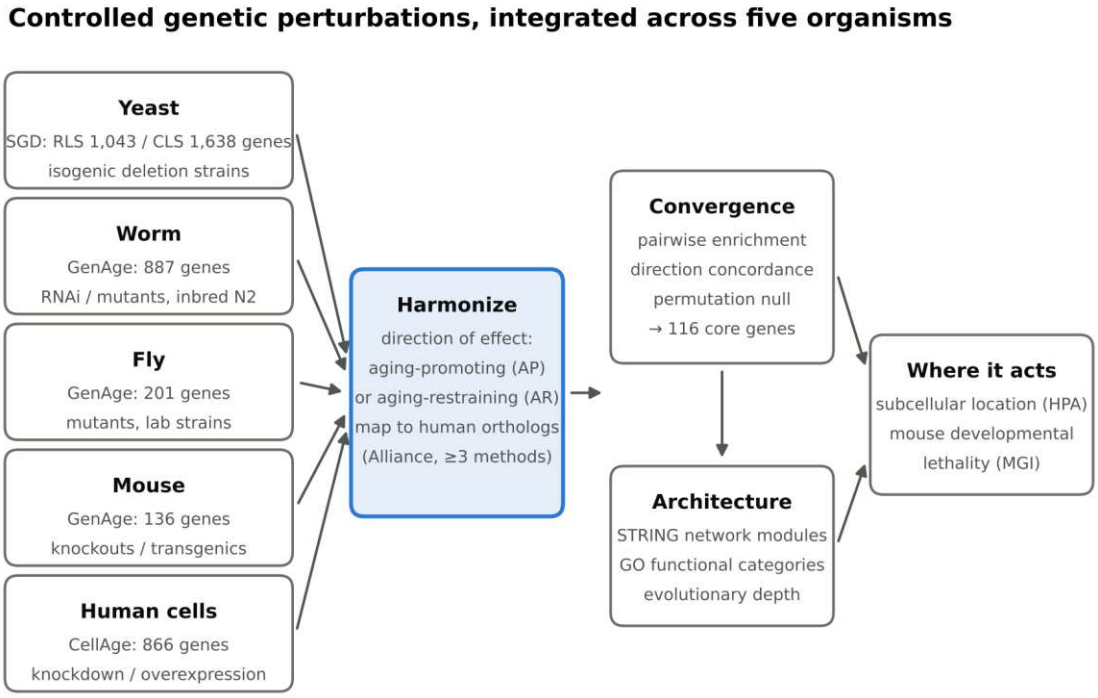


Fig. 1 Study design. Genetic perturbations measured against a defined genetic background in five systems were coded by direction (aging-promoting or aging-restraining), mapped to human orthologs, and tested for convergence, network structure, functional category, subcellular location and requirement for development.

The integrated catalog comprised 4,771 single-gene effects mapping to 3,399 distinct human genes (Table 1; Fig. 1; Supplementary Table S7). Directional composition differed across assays. Aging-promoting classifications predominated in nematode and yeast replicative lifespan datasets, consistent with the contribution of loss-of-function screens identifying lifespan extension. Aging-restraining classifications predominated in fruit fly, mouse, yeast chronological lifespan and human-cell datasets. These distributions reflect both biological effects and differences in experimental design and ascertainment.

3.2 Cross-species convergence of longevity regulators without uniform directional concordance

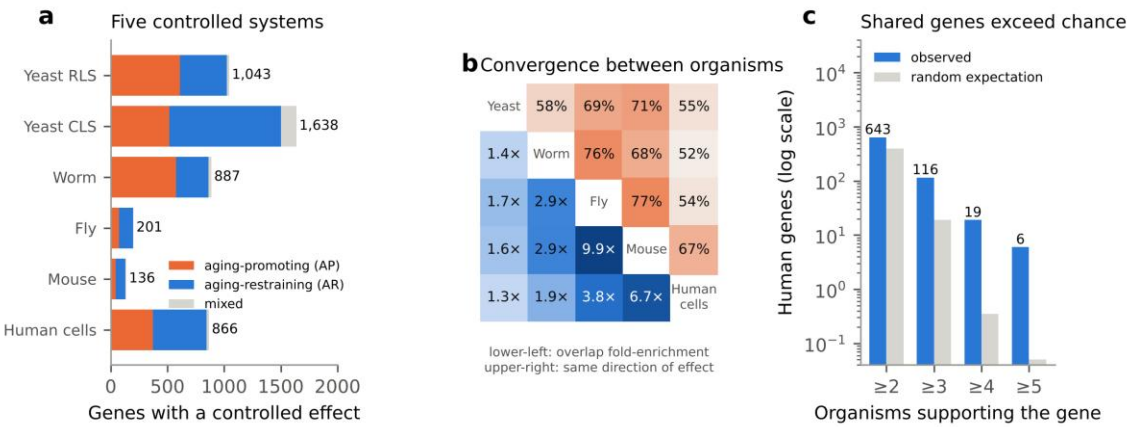


Fig. 2 Controlled experiments in different organisms converge on shared genes. (a) Genes with a controlled effect in each system, split by direction. (b) Lower-left cells: fold-enrichment of the overlap between two organisms' aging genes relative to chance, within their shared ortholog universe (all $P < 0.001$). Upper-right cells: share of overlapping genes that act in the same direction in both organisms. (c) Number of human genes supported by at least 2, 3, 4 or 5 organisms, observed and expected from 1,000 random draws (log scale).

Every pair of organisms shared more aging-associated genes than expected, ranging from 1.3-fold for yeast and human cells to 9.9-fold for flies and mice (all $P < 0.001$; Table 2, Fig. 2b). Overlaps remained enriched when yeast evidence was restricted to genome-wide, hypothesis-free deletion screens (1.3- to 1.5-fold; all $P \leq 0.012$; Supplementary Table S3), indicating that convergence does not arise solely from candidate genes selected on the basis of findings in another organism. One hundred and sixteen human genes exhibited controlled effects in at least three organisms, compared with 19.0 expected (6.1-fold; permutation $P = 0.001$, the minimum attainable with 1,000 permutations), and six exhibited effects in all five (0.002 expected): RPS6KB1, MTOR, TXN, SIRT1, FXN and SOD2 (Fig. 2c).

Table 2. Pairwise convergence of controlled aging genes (human-ortholog level)

Pair	Shared universe	Genes A / B	Overlap (expected)	Fold	Same direction	Binomial P
Yeast – Worm	3,428	1,452 / 536	307 (227.0)	1.4	139 / 241 (58%)	0.010
Yeast – Fly	3,571	1,494 / 114	81 (47.7)	1.7	38 / 55 (69%)	0.003
Yeast – Mouse	4,014	1,715 / 46	31 (19.7)	1.6	20 / 28 (71%)	0.018
Worm – Fly	7,678	1,045 / 225	88 (30.6)	2.9	60 / 79 (76%)	2×10^{-6}
Worm – Mouse	8,754	1,123 / 81	30 (10.4)	2.9	17 / 25 (68%)	0.054
Fly – Mouse	9,924	283 / 92	26 (2.6)	9.9	20 / 26 (77%)	0.005

Pair	Shared universe	Genes A / B	Overlap (expected)	Fold	Same direction	Binomial P
Yeast – Human cells	4,107	1,744 / 268	146 (113.8)	1.3	66 / 121 (55%)	0.18
Worm – Human cells	8,964	1,140 / 555	132 (70.6)	1.9	60 / 116 (52%)	0.39
Fly – Human cells	10,141	284 / 623	67 (17.4)	3.8	36 / 67 (54%)	0.31
Mouse – Human cells	18,133	147 / 859	47 (7.0)	6.7	30 / 45 (67%)	0.018

All overlaps P < 0.001 (one-sided Fisher's exact test). Expected overlap in parentheses. Same direction: share of overlapping genes with a resolved directional annotation in both organisms that act the same way; binomial P values are unadjusted (Benjamini–Hochberg q-values in Supplementary Table S8).

These results confirm, with identifier-based orthology and explicit bias controls, the convergence reported in earlier comparative analyses (Smith et al. 2008; Yanai et al. 2017). Direction of effect, however, was less uniform. Among whole organisms, 58–77% of shared genes acted in the same direction (five of six pairs significant; Benjamini–Hochberg q ≤ 0.03). Agreement between human cellular senescence and yeast, nematode or fly lifespan was 52–55% (P ≥ 0.18), and agreement between human cells and mice was 67% (P = 0.018). Shared gene identity therefore does not imply a shared direction of effect; the following sections identify the conditions under which direction is conserved.

3.3 Directional conservation of longevity regulators between experimental systems

Three analyses of directional conservation were applied to the harmonized catalog (Table 3, Fig. 3).

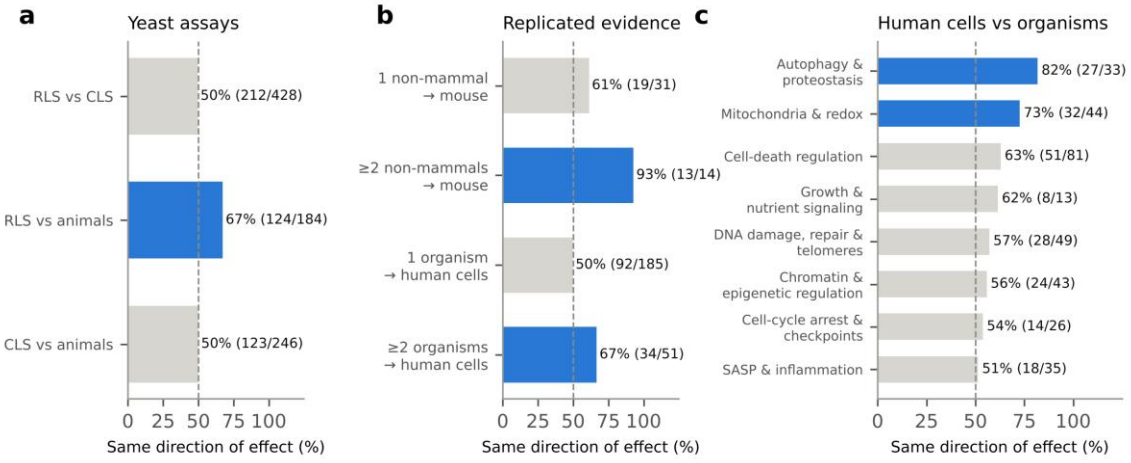


Fig. 3 Directional conservation of longevity regulators between experimental systems. Bars show the proportion of genes with a resolved direction in both systems that act in the same direction; the dashed line marks chance (50%); counts denote same-direction genes over genes compared. Blue bars differ from 50% (two-sided binomial P < 0.05; in panel c, Benjamini–Hochberg q < 0.05 across the eight categories). (a) Yeast replicative (RLS) and chronological (CLS) lifespan compared with each other and

with the consensus direction in nematodes, flies and mice. (b) Agreement with the mouse direction when one, or at least two concordant, non-mammalian organisms (yeast, nematode, fly) support a gene, and agreement of human-cell senescence with the organismal consensus when that consensus rests on one or on at least two organisms. (c) Agreement of human-cell senescence with the organismal consensus by functional category.

Table 3. Directional conservation between experimental systems

Comparison	Genes compared	Same direction	P
Yeast RLS vs yeast CLS (human-ortholog level)	428	212 (50%)	0.89
Yeast RLS vs yeast CLS (yeast-gene level)	402	216 (54%)	0.15
Yeast RLS vs animal consensus (nematode, fly, mouse)	184	124 (67%)	3×10^{-6}
Yeast CLS vs animal consensus (nematode, fly, mouse)	246	123 (50%)	1.0
Mouse vs ≥ 2 concordant non-mammalian organisms	14	13 (93%)	0.002
Mouse vs one non-mammalian organism	31	19 (61%)	0.28
Human cells vs organismal consensus, all genes	236	126 (53%)	0.33
Human cells vs consensus from one organism	185	92 (50%)	1.0
Human cells vs consensus from ≥ 2 organisms	51	34 (67%)	0.024

Genes compared: genes with a resolved aging-promoting or aging-restraining direction in both systems. P: two-sided binomial test against 50%. Non-mammalian organisms: yeast, nematode and fly. Concordant versus single non-mammalian evidence for the mouse direction: odds ratio 8.2, Fisher's exact P = 0.038; consensus from ≥ 2 versus one organism for human cells: odds ratio 2.0, P = 0.039. Yeast directions in the mouse and human-cell rows pool RLS and CLS. Source data: Supplementary Table S10.

3.3.1 Replicative, but not chronological, yeast lifespan predicts the direction of effect in animals

Yeast replicative and chronological lifespan shared regulators far more often than expected (511 human genes versus 296.4 expected; 1.7-fold; $P = 2 \times 10^{-63}$); nevertheless, of the 428 shared genes with a resolved direction in both assays, only 212 (50%) acted in the same direction (P = 0.89; Table 3, Fig. 3a). The result was unchanged without ortholog mapping (216 of 402 yeast genes, 54%; P = 0.15). SIR2, for example, was aging-restraining for replicative and aging-promoting for chronological lifespan. The two assays also differed markedly in their concordance with animals. Replicative lifespan agreed with the consensus direction in nematodes, flies and mice for 124 of 184 genes (67%; $P = 3 \times 10^{-6}$), whereas chronological lifespan agreed for 123 of 246 (50%; P = 1.0). The yeast–animal concordance reported in Table 2 therefore appears to derive from replicative lifespan.

3.3.2 Concordant non-mammalian evidence predicts the direction of effect in mice

For 14 genes with a resolved mouse lifespan direction, at least two of yeast, nematode and fly had resolved and concordant directions. The mouse direction matched in 13 of these (93%; P = 0.002; Fig. 3b); the sole exception was SLC25A4, aging-promoting in yeast and nematodes but aging-restraining in mice. When only one non-mammalian organism had a resolved direction, the mouse direction matched in 19 of 31 genes (61%; P = 0.28; concordant versus single-organism evidence, odds ratio 8.2, P = 0.038). After human paralogs mapping to the same non-human genes were collapsed, 12 of 13 independent gene groups remained concordant. Because the replicated set comprises some of the most intensively studied aging regulators (MTOR, RPS6KB1, IGF1R, INSR, PTEN and SIRT1), the 93% figure is best regarded as an upper estimate of predictive accuracy. Multi-organism evidence likewise improved concordance with human cells: CellAge genes whose organismal consensus rested on two or more organisms agreed in 34 of 51 cases (67%; P = 0.024), compared with 92 of 185 (50%; P = 1.0) when it rested on one (odds ratio 2.0; P = 0.039).

Applying the replication criterion to genes not yet examined in mice nominates 180 human genes, corresponding to 112 groups of non-human source genes, that show concordant effects in at least two non-mammalian organisms and possess a mouse ortholog but lack controlled mouse lifespan data (92 aging-promoting, 88 aging-restraining; Supplementary Table S9). Twelve genes in nine source-gene groups had concordant support in all three non-mammalian organisms: the autophagy genes ATG3, GABARAP and VPS33A, the endoplasmic-reticulum stress sensors ERN1 and ERN2, the peroxiredoxin PRDX2 and the forkhead factor FOXA1 (aging-restraining), and the S6 kinase paralog RPS6KB2 and the SLC13A2–SLC13A5 sodium-coupled sulfate/dicarboxylate transporters (aging-promoting). These genes constitute directly testable predictions for mouse lifespan.

3.3.3 Directional conservation between cellular senescence and organismal lifespan is confined to maintenance functions

Agreement between human-cell senescence and organismal lifespan was at chance overall (126 of 236 genes, 53%; P = 0.33) but varied substantially with function (Table 4, Fig. 3c). Agreement was high for autophagy and proteostasis genes (27 of 33, 82%; q = 0.003) and mitochondrial and redox genes (32 of 44, 73%; q = 0.015), intermediate for cell-death regulators (51 of 81, 63%; q = 0.07), and at chance for chromatin, DNA-damage, cell-cycle arrest and SASP/inflammation genes (51–57%; q ≥ 0.77). After genes assigned to both groups were excluded, maintenance genes agreed in 33 of 45 cases (73%) and arrest or SASP genes in 17 of 41 (41%; odds ratio 3.9; P = 0.004). Disagreement did not reflect a systematic reversal of sign: of 110 discordant genes, 59 promoted senescence while restraining organismal aging, and 51 showed the converse pattern (P = 0.50). Growth-signaling genes had too few resolved pairs (8 of 13 concordant) for a reliable estimate.

Table 4. Functional categories: organismal coverage and directional conservation of human senescence genes

Functional category	Genes in genome	Core genes	CellAge genes	With organismal lifespan evidence	With a yeast ortholog	Same direction, cells vs organisms (q)

Functional category	Genes in genome	Core genes	CellAge genes	With organismal lifespan evidence	With a yeast ortholog	Same direction, cells vs organisms (q)
Growth and nutrient signaling	109	14	20	80%	40%	8/13, 62% (0.77)
Mitochondria and redox	779	36	90	54%	43%	32/44, 73% (0.015)
Autophagy and proteostasis	986	18	85	44%	52%	27/33, 82% (0.003)
Cell-death regulation	1,272	50	227	43%	30%	51/81, 63% (0.07)
Chromatin and epigenetic regulation	769	21	135	41%	44%	24/43, 56% (0.77)
DNA damage, repair and telomeres	771	20	149	40%	43%	28/49, 57% (0.77)
Cell-cycle arrest and checkpoints	320	11	81	36%	38%	14/26, 54% (0.97)
SASP and inflammation	991	14	116	35%	22%	18/35, 51% (1.00)

Categories derived from Gene Ontology biological-process annotations (GOA human, with ancestor terms); a gene may belong to several categories. With organismal lifespan evidence: proportion of CellAge genes in the category whose ortholog has a controlled lifespan effect in yeast, nematode, fly or mouse. Same direction: CellAge genes whose senescence direction matches the organismal consensus, out of those with a resolved direction in both; q, Benjamini–Hochberg-adjusted two-sided binomial P across the eight categories.

Arrest and inflammatory senescence genes were also less frequently represented in organismal datasets. Among human senescence genes assigned to growth and nutrient signaling, 80% had organismal lifespan evidence, compared with 36% for cell-cycle arrest and checkpoints ($P = 7 \times 10^{-4}$) and 35% for SASP and inflammation ($P = 3 \times 10^{-4}$); 22% of SASP/inflammation genes had a yeast ortholog, compared with 52% of autophagy/proteostasis genes (Table 4). Arrest and inflammatory senescence regulators are therefore both less extensively sampled in organisms and, where sampled, uninformative about the organismal direction of effect. CDKN2A, RB1, RELA, IL6 and GATA4, for example, lacked controlled lifespan annotations in all four non-human systems.

3.4 Composition of the 116-gene conserved core

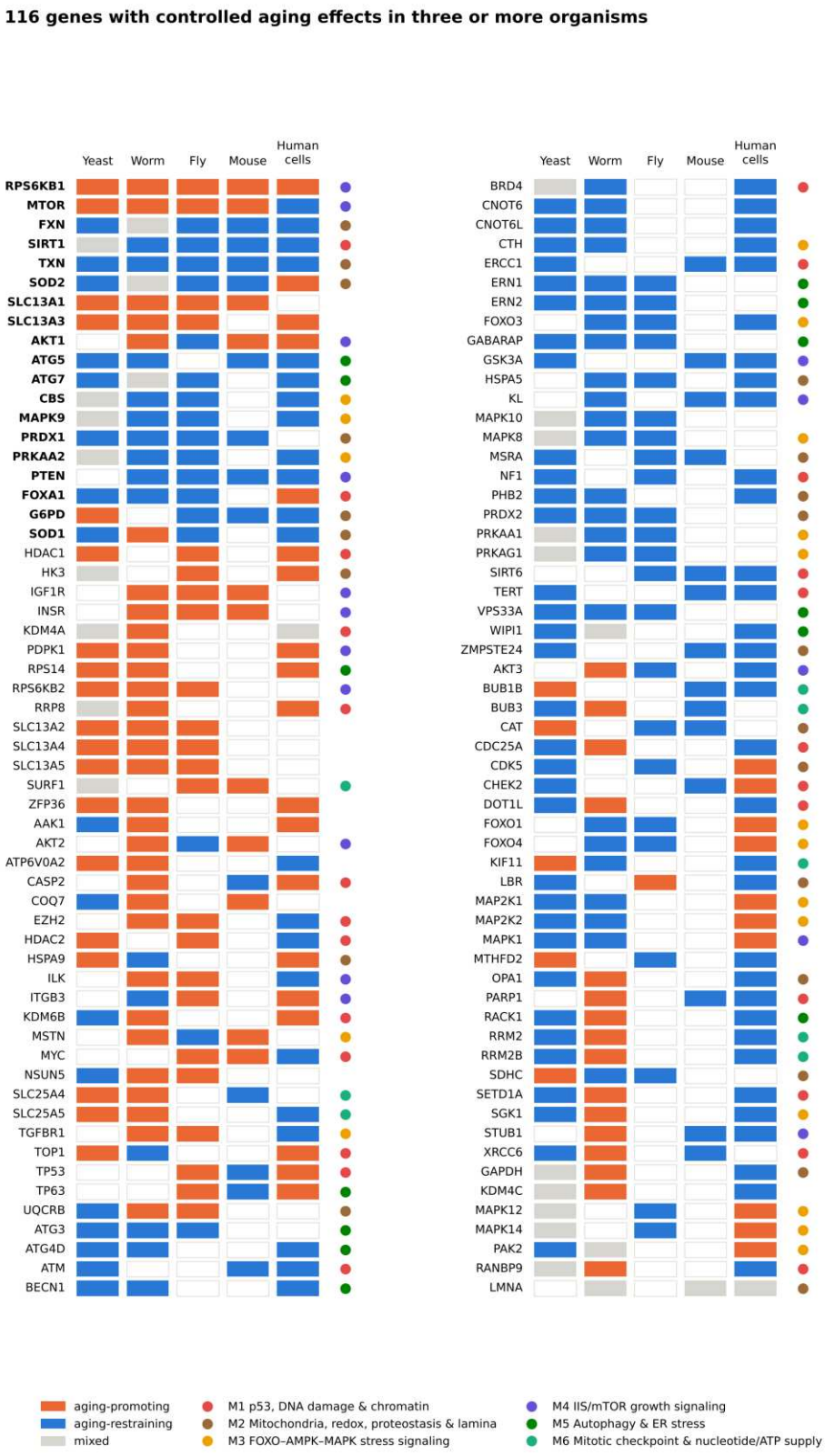


Fig. 4 The 116 core genes and their direction of effect in each organism. Each row is a human gene; each column an organism in which its ortholog was tested under controlled conditions. Orange, aging-promoting; blue, aging-restraining; gray, mixed; empty, no controlled data. Bold names are supported by four or five organisms. Colored dots give the network module (Fig. 5).

Among the 116 core genes, consensus classifications were aging-restraining for 69, aging-promoting for 40 and mixed for seven (Fig. 4; Supplementary Table S1). Fifty-six genes acted in the same direction in every system with a resolved annotation. Nineteen genes had evidence in four or five systems (Table 5); these encompass growth and nutrient signaling (RPS6KB1, MTOR, AKT1, PTEN), energy and stress sensing (PRKAA2, MAPK9, SIRT1), autophagy (ATG5, ATG7), and redox and mitochondrial metabolism (TXN, PRDX1, SOD1, SOD2, FXN, G6PD, CBS). MTOR was aging-promoting in yeast, nematodes, flies and mice but aging-restraining in human cells, and SOD2 was aging-promoting in human cells alone, exemplifying the cell–organism discordance quantified above.

Table 5. Genes with controlled aging effects in four or five organisms

Gene	Yeast	Worm	Fly	Mouse	Human cells	Consensus	Molecular function
RPS6KB1	AP	AP	AP	AP	AP	AP (5/5)	S6 kinase 1; mTORC1 effector driving translation
MTOR	AP	AP	AP	AP	AR	AP (4/5)	TOR kinase; growth and nutrient signaling
TXN	AR	AR	AR	AR	AR	AR (5/5)	Thioredoxin; redox control
SIRT1	mixed	AR	AR	AR	AR	AR (4/4)	NAD^+-dependent deacetylase; yeast Sir2 family
FXN	AR	mixed	AR	AR	AR	AR (4/4)	Frataxin; mitochondrial iron–sulfur cluster assembly
SOD2	AR	mixed	AR	AR	AP	AR (3/4)	Mitochondrial superoxide dismutase
AKT1	–	AP	AR	AP	AP	AP (3/4)	AKT kinase; insulin/IGF signaling to TOR
ATG5	AR	AR	–	AR	AR	AR (4/4)	Autophagy core; ATG12–ATG5 conjugate
ATG7	AR	mixed	AR	–	AR	AR (3/3)	Autophagy core; E1-like enzyme
CBS	mixed	AR	AR	–	AR	AR (3/3)	Cystathionine β-synthase; transsulfuration

Gene	Yeast	Worm	Fly	Mouse	Human cells	Consensus	Molecular function
FOXA1	AR	AR	AR	–	AP	AR (3/4)	Forkhead transcription factor family
G6PD	AP	–	AR	AR	AR	AR (3/4)	Glucose-6-phosphate dehydrogenase; NADPH supply
MAPK9	mixed	AR	AR	–	AR	AR (3/3)	JNK2 stress kinase
PRDX1	AR	AR	AR	AR	–	AR (4/4)	Peroxiredoxin 1; peroxide detoxification
PRKAA2	mixed	AR	AR	–	AR	AR (3/3)	AMPK catalytic α2 subunit; energy sensing
PTEN	–	AR	AR	AR	AR	AR (4/4)	Lipid phosphatase opposing PI3K–AKT
SLC13A1	AP	AP	AP	AP	–	AP (4/4)	Sodium-coupled sulfate/dicarboxylate transporter family
SLC13A3	AP	AP	AP	–	AP	AP (4/4)	Sodium-coupled dicarboxylate transporter
SOD1	AR	AP	AR	–	AR	AR (3/4)	Cu/Zn superoxide dismutase

AP, aging-promoting; AR, aging-restraining; –, no controlled data. Rows are ordered by the number of organisms, then alphabetically. Consensus gives the number of organisms agreeing out of those with a resolved directional annotation. Orthologs map one-to-many in some families (for example, several human SLC13A, AKT and PRKAA genes share one fly or worm ortholog).

3.5 Network organization of the core and convergence with cell-death and autophagy pathways

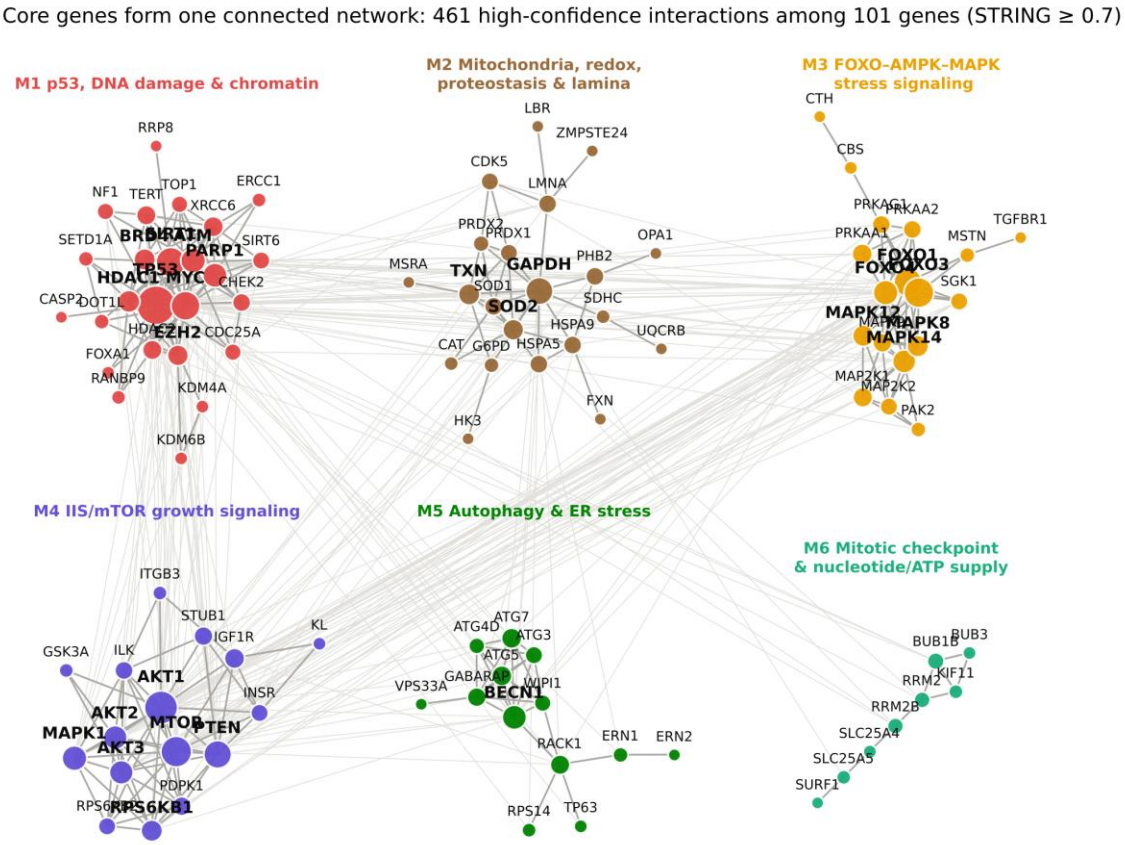


Fig. 5 The core genes form one interconnected network with six modules. Nodes are the 101 core genes in the main connected component of the STRING network (combined score ≥ 0.7); node size reflects the number of connections and color the Louvain module. Dark gray lines connect genes within a module, light lines between modules. Not shown: MAPK10 (no STRING entry), 11 genes with no high-confidence partner, and one small component of three genes.

Of the 116 core genes, 115 mapped to STRING, yielding 464 high-confidence associations compared with 148 expected (STRING enrichment $P \approx 10^{-64}$). A connected component of 101 genes resolved into six communities in the seed-1 Louvain solution (Fig. 5; Table 6). The most highly connected nodes were TP53 (degree 54), AKT1 (38), MTOR (32), FOXO3 (30), SIRT1 (29) and MYC (28). Community structure varied across 100 random seeds (four to seven modules; mean adjusted Rand index 0.77 relative to seed 1), most often through merging of the FOXO–AMPK–MAPK and insulin/IGF–TOR communities; the modules are therefore best interpreted as overlapping functional neighborhoods. STRING associations do not, by themselves, establish direct binding or the direction of regulation.

Table 6. Network modules of the core cell-aging genes

Module	Genes	Hub genes	Consensus direction (AR / AP / mixed)	Main locations (HPA)	Mouse knockout lethal
M1 p53, DNA damage and chromatin	25	TP53, SIRT1, MYC, ATM	14 / 10 / 1	Nucleus 96%, cytosol 20%	83% (20/24)
M2 Mitochondria, redox, proteostasis and nuclear lamina	21	GAPDH, TXN, SOD2, SOD1	16 / 3 / 2	Nucleus 47%, cytosol 47%, mitochondria 35%	71% (15/21)
M3 FOXO–AMPK–MAPK stress signaling	18	FOXO3, FOXO1, FOXO4, MAPK14	13 / 2 / 3	Nucleus 81%, cytosol 69%	33% (6/18)
M4 Insulin/IGF–TOR growth signaling	16	AKT1, MTOR, PTEN, MAPK1	6 / 10 / 0 (growth kinases AP; PTEN, GSK3A, KL, STUB1, AKT3, MAPK1 AR)	Nucleus 73%, cytosol 67%	62% (10/16)
M5 Autophagy and ER stress	13	BECN1, ATG5, ATG7, RACK1	11 / 2 / 0	Nucleus 58%, cytosol 58%, vesicles 17%	73% (8/11)
M6 Mitotic checkpoint and nucleotide/ATP supply	8	BUB1B, RRM2B, RRM2, KIF11	5 / 3 / 0	Cytosol 57%, nucleus 43%, mitochondria 29%	71% (5/7)

AR, aging-restraining; AP, aging-promoting. Hub genes are the four most connected genes in each module (ties: HSPA9 and LMNA share SOD1's degree of 8 in M2; SLC25A5 shares KIF11's degree of 3 in M6). Locations are the share of genes with Human Protein Atlas immunofluorescence data that are detected in that compartment (main or additional location; a gene may be in several). Lethality is the share of genes with recorded mouse knockout phenotypes that show embryonic, perinatal or preweaning lethality.

Relative to the genome, the core was enriched for cellular response to stress (67 genes; $P = 1 \times 10^{-37}$), programmed cell death (65 genes; $P = 8 \times 10^{-34}$), FoxO signaling (28 genes; $P = 4 \times 10^{-27}$), autophagy (26 genes; $P = 2 \times 10^{-21}$) and cellular senescence (16 genes; $P = 2 \times 10^{-16}$) (Supplementary Table S2). FoxO signaling ($P = 7 \times 10^{-17}$), programmed cell death ($P = 1 \times 10^{-15}$) and autophagy ($P = 4 \times 10^{-12}$) remained enriched against the stringent background of all 3,399 aging-associated genes. Autophagy displayed the most uniform direction in the catalog: among 24 autophagy-core genes (ATG proteins, ULK1/2, BECN1, WIPI and GABARAP/LC3 families), 46 of 47 directionally resolved gene–system observations were aging-

restraining, compared with 52% across the entire catalog (Supplementary Table S8); ATG10 in human cells was the sole exception.

3.6 Subcellular localization and developmental essentiality

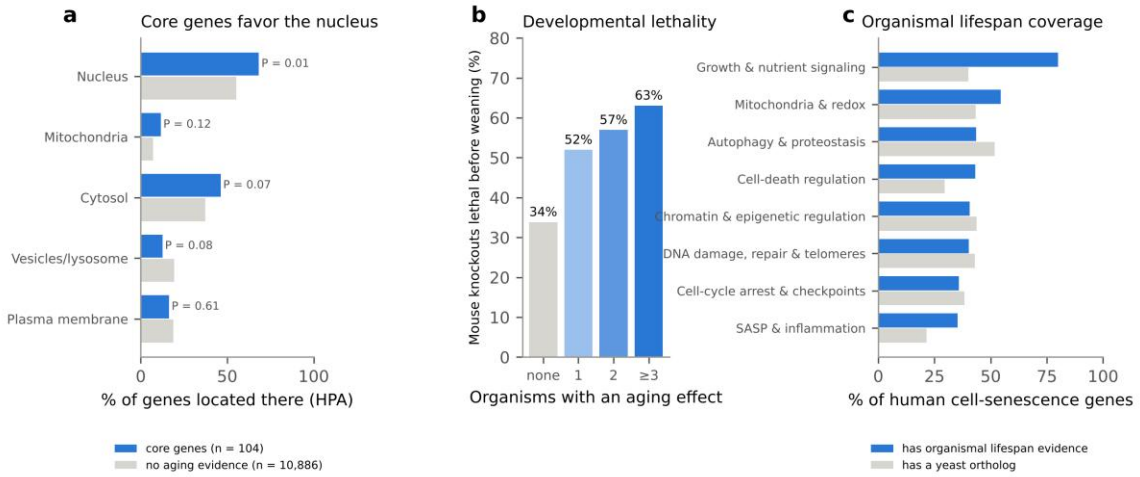


Fig. 6 Where and when the cell-aging genes act. (a) Subcellular location (Human Protein Atlas) of core genes compared with genes with no aging evidence; P from Fisher's exact test. (b) Share of mouse knockouts that die before weaning, by the number of organisms in which the gene affects aging. (c) For human cell-senescence genes (CellAge) in each functional category, the share whose orthologs also change organism lifespan in yeast, worm, fly or mouse (blue) and the share that have a yeast ortholog (gray).

Core genes were more frequently nuclear than genes lacking catalogd aging evidence (68% versus 55%; P = 0.007), with no significant difference in mitochondrial, cytosolic, vesicular or plasma-membrane localization (Fig. 6a; Supplementary Table S4). Module-level localization was consistent with function: 96% of annotated M1 genes (p53, DNA damage and chromatin) were nuclear, and M2 (mitochondria, redox and proteostasis) had the highest mitochondrial proportion (35%).

Among genes with recorded mouse knockout phenotypes, lethality before weaning occurred for 34% of genes without aging evidence, 52% of genes supported in one system, 57% of those supported in two and 63% of core genes (Fig. 6b). After adjustment for the number of phenotyped single-gene mouse genotypes, aging-associated genes as a group retained higher odds of developmental lethality (odds ratio 1.89; 95% CI 1.73–2.07; P < 0.001), whereas core status conferred no significant additional association (odds ratio 1.45; 95% CI 0.95–2.23; P = 0.09; Supplementary Table S5).

Antagonistic pleiotropy predicts that aging-promoting genes are preferentially required early in life. The direction-resolved data showed the opposite pattern. Among aging genes with a resolved direction, knockout lethality was more frequent for aging-restraining genes (57%, n = 1,320) than for aging-promoting genes (48%, n = 1,188; odds ratio 1.40; P < 0.001). The difference was attributable to human-cell senescence genes (68% vs 52%, aging-restraining vs aging-promoting) and yeast chronological lifespan genes (59% vs 49%); yeast replicative lifespan genes showed a non-significant trend in the same direction (54% vs 47%; P = 0.07), nematode and mouse genes showed no difference, fly genes showed a

non-significant opposite trend (43% vs 54%; P = 0.08), and core genes showed similar proportions (60% vs 64%) (Supplementary Table S6).

4. Discussion

4.1 Advances beyond previous comparative analyses

Earlier comparative analyses established that genes affecting lifespan in one model organism are enriched among the aging-associated genes of another (Budovsky et al. 2007; Smith et al. 2008; Yanai et al. 2017) and that senescence regulators overlap longevity genes (Avelar et al. 2020). The present study reproduces these observations and extends them in a direction-resolved framework, converting catalogs of shared genes into explicit criteria for the use of model-organism evidence: which yeast assay to rely on, what degree of cross-species replication predicts a mammalian outcome, and which human senescence regulators have organismal counterparts. Each criterion is quantified within a single harmonized catalog and generates testable predictions.

Several design features strengthen these inferences. Orthologs were assigned by database identifier rather than gene symbol, which recovered outdated GenAge nomenclature that symbol matching would have omitted. Convergence persisted when yeast evidence was restricted to hypothesis-free genome-wide screens, and the association with developmental essentiality was adjusted for mouse phenotyping intensity. Paralog families were collapsed to independent source-gene groups in the replication analysis, and false-discovery-rate control was applied to the pairwise and category-level concordance tests.

4.2 Replicative lifespan as the phylogenetically informative yeast assay

Replicative and chronological lifespan share regulators but not the direction of their effects, indicating that the two assays capture distinct biology. Replicative lifespan reflects the division potential of a mother cell and is constrained by mechanisms that include rDNA instability and loss of Sir2-dependent silencing (Mortimer and Johnston 1959; Sinclair and Guarente 1997; Kaeberlein et al. 1999). Chronological lifespan measures the survival of non-dividing cells in stationary culture and is highly sensitive to medium composition, auxotrophy and strain background; independent genome-wide CLS screens show little mutual overlap (Smith et al. 2016). In the present catalog, CLS direction conveyed no information about the direction of animal lifespan effects, whereas RLS direction did. Chronological aging may nonetheless model non-dividing or quiescent cells more faithfully than whole-organism lifespan. For inferences concerning animal lifespan, however, the two yeast assays should not be pooled, and replicative lifespan is the more informative assay.

4.3 Cross-species replication as a predictive criterion for mammalian studies

Concordance between two or more non-mammalian organisms predicted the mouse direction in 13 of 14 genes, whereas evidence from a single organism performed little better than chance. The 180 untested candidates (Supplementary Table S9) provide a prospective test of this criterion: if cross-species replication is predictive, their mouse mutants should display the predicted direction more often than single-organism candidates. RPS6KB2 is a particularly informative candidate, because loss of its paralog S6K1 extends mouse lifespan (Selman et al. 2009). Many candidates are required for development (72 of the 159 with recorded mouse knockout phenotypes die before weaning; Supplementary Table S9) and would therefore require conditional or adult-onset alleles.

4.4 Maintenance functions as the interface between cellular senescence and organismal aging

Avelar et al. (2020) showed that senescence genes are conserved in mammals but much less so in invertebrates. The present analysis extends this observation: even when a senescence regulator has an organismal lifespan annotation, its direction is conserved most reliably when it functions in autophagy, proteostasis or mitochondrial and redox maintenance. Arrest and SASP genes agreed only at chance, and their disagreement did not represent a consistent sign reversal. These findings are difficult to reconcile with a simple model in which senescence-inducing genes uniformly extend organismal lifespan through tumor suppression, or uniformly shorten it through inflammatory secretion; both effects are documented (Serrano et al. 1997; Coppé et al. 2008), and which prevails appears to depend on the gene and the physiological context. Accordingly, human-cell senescence screens are most informative about organismal aging for maintenance genes, whereas arrest and SASP regulators require direct organismal testing.

4.5 Developmental essentiality and antagonistic pleiotropy

Yanai et al. (2017) noted that essential longevity genes are highly conserved and proposed that antagonistic pleiotropy may represent a conserved principle of aging. A specific formulation of this hypothesis predicts that aging-promoting genes should be those required for development. The direction-resolved data did not support this prediction: aging-restraining genes were more frequently lethal when inactivated in mice than aging-promoting genes, and core status did not significantly augment the excess essentiality of aging-associated genes after adjustment for study intensity. Development thus depends on the maintenance genes that restrain aging at least as much as on the growth-promoting genes that accelerate it. Because developmental lethality captures only one component of early-life fitness, this result constrains a specific formulation of antagonistic pleiotropy rather than the broader hypothesis or the developmental-hyperfunction model.

4.6 A conserved regulatory architecture of cellular aging

The core genes define a regulatory architecture with three interacting layers (Fig. 7). Nutrient and growth-factor signaling, comprising TOR–S6K in all systems and insulin/IGF–AKT in animals, sets biosynthetic demand; AMPK, FOXO, PTEN, sirtuins and stress-response regulators modulate this signaling; and autophagy, redox defense, proteostasis and genome and chromatin maintenance preserve cellular function. Mammalian arrest and inflammatory pathways contribute context-dependent senescence outputs. The analyses of directional conservation map onto this architecture: the maintenance layers are directionally conserved across systems, whereas the senescence outputs diverge.

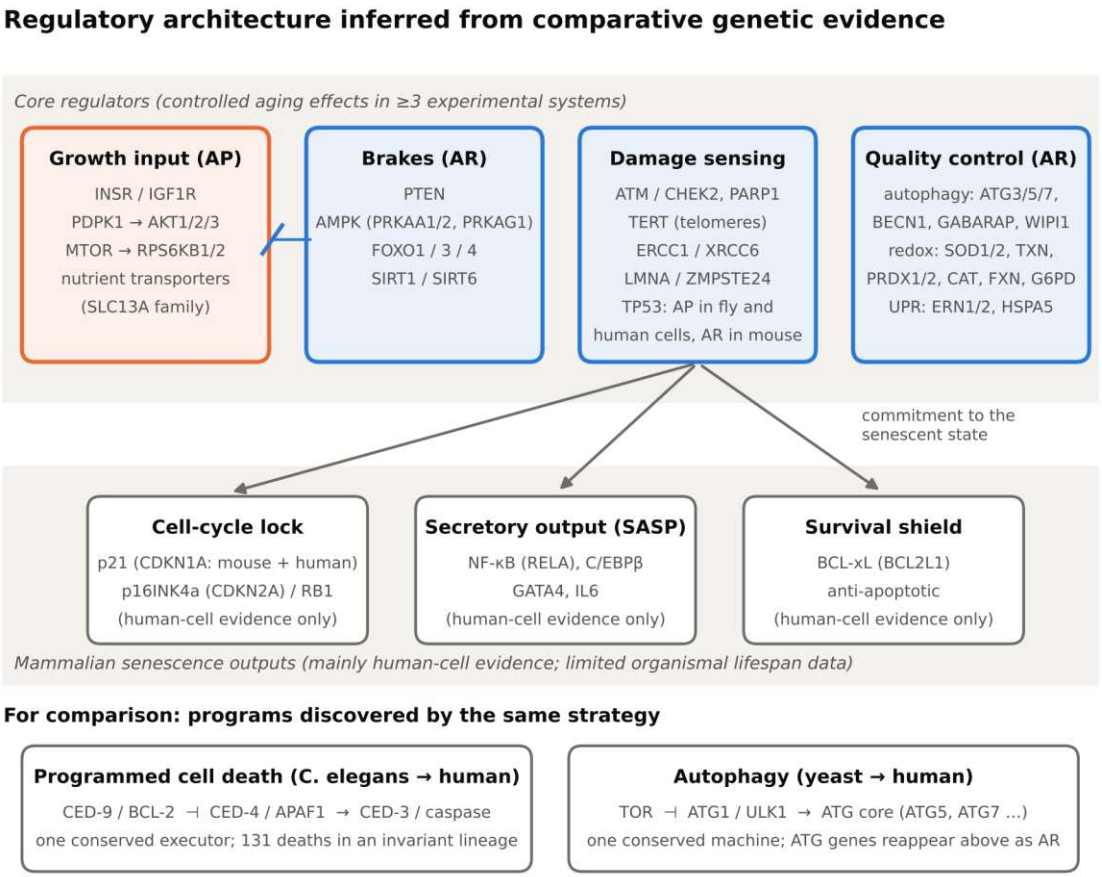


Fig. 7 Regulatory architecture inferred from comparative genetic evidence. Top: core regulators grouped by annotated biological roles; orange indicates aging-promoting and blue aging-restraining classifications. Middle: mammalian senescence-associated effectors with predominantly human-cell evidence; CDKN1A also has mouse support, and CEBPB has a mixed mouse annotation. Bottom: cell-death and autophagy pathways shown for functional comparison. The diagram is a conceptual synthesis rather than a directly measured causal wiring map. Maintenance layers are directionally conserved across systems (Fig. 3), whereas senescence outputs diverge. Absence of an organismal lifespan annotation denotes an evidence gap.

Programmed cell death and autophagy possess dedicated executors, the caspases and the ATG machinery, that were defined genetically (Ellis and Horvitz 1986; Yuan et al. 1993; Tsukada and Ohsumi 1993). The present catalog identifies no aging-specific executor (Table 7). Its overlap with cell death lies upstream, in TP53, AKT1, FOXO factors, PTEN and sirtuins; APAF1 and CASP9 lacked lifespan annotations, and CASP2 was the only caspase in the core. Autophagy, by contrast, was uniformly aging-restraining, consistent with its role in cellular and tissue homeostasis (Mizushima and Komatsu 2011). The term “program” is therefore used here in a regulatory sense, denoting an interacting set of gene-encoded regulators whose activity is tuned by nutrients, stress and cellular history, for example through amino-acid and energy control of mTORC1 and ULK1 (Sancak et al. 2008; Kim et al. 2011), rather than a deterministic timetable. Variation in aging among isogenic individuals (Herndon et al. 2002; Rea et al.

2005) is consistent with this interpretation. These conclusions pertain to the fungal and animal lineages examined here; extending the framework to plants and to long-lived vertebrates is a natural next step.

Table 7. Three cellular programs compared

Feature	Programmed cell death	Autophagy	Cell aging (this study)
Founding system	*C. elegans* invariant lineage	Yeast under starvation	Yeast mother cells, isogenic worms, flies, mice; human cells in culture
Founding screen	Mutants with persistence of normally eliminated cells	Mutants unable to form autophagic bodies	Targeted genetic perturbations altering lifespan or senescence
Outcome	Cell elimination; stereotyped developmental timing in the founding model	Intracellular turnover responsive to nutrients and stress	Gradual loss of function; permanent arrest in mammalian cells
Core genes	*ced-3*, *ced-4*, *ced-9*, *egl-1*	About 15 complementation groups (*APG/ATG*)	116 genes in ≥ 3 organisms; 19 in ≥ 4
Dedicated executor	Caspase-dependent execution	ATG-dependent autophagosome biogenesis	No aging-specific executor identified in this catalog
Conserved to humans	Yes	Yes	Conserved signaling and maintenance; more limited yeast orthology for inflammatory outputs
Timing	Lineage-dependent in developmental apoptosis; context-dependent in other settings	Responsive to nutrient status and cellular stress	Regulated by growth–maintenance interactions and cellular and environmental context

5. Conclusions

The sharing of aging-associated genes among yeast, nematodes, flies, mice and human cells is well established; this study defines the conditions under which their direction of effect is conserved and identifies three governing principles. First, yeast replicative lifespan, but not chronological lifespan, carries directional information about animal lifespan; the two yeast assays share regulators but not

effect direction. Second, concordance between two or more non-mammalian organisms predicted the mouse direction in 13 of 14 genes, and the same criterion nominates 180 human genes, including ATG3, GABARAP, VPS33A, PRDX2 and RPS6KB2, for mouse lifespan studies. Third, human senescence regulators predict the organismal direction of effect when they function in autophagy, proteostasis or mitochondrial and redox maintenance, but not when they function in cell-cycle arrest or inflammatory secretion.

Direction-resolved data further show that aging-restraining genes, rather than aging-promoting genes, constitute the more developmentally essential class, contrary to a specific antagonistic-pleiotropy prediction. Most of the 116 genes shared by at least three systems form a single network linking nutrient signaling to autophagy, redox and chromatin maintenance. Together, these results describe an evolutionary architecture of longevity regulation in which maintenance functions are directionally conserved across species, whereas senescence outputs have diverged.

Statements and Declarations

Funding No funding was received for conducting this study or for the preparation of this manuscript.

Competing interests The author has no relevant financial or non-financial interests to disclose. The author was previously employed by the USDA Food Safety and Inspection Service (until 2025); this work was conducted independently, used no non-public agency data, and does not represent the views of the USDA.

Author contributions D.W.C. conceived the study, defined the research strategy and questions, collected the main data, performed the analyses, and wrote the manuscript. More data retrieval, coding, and figure drafts were carried out with AI assistance under the author's direction (Section 2.10).

Data availability All data analyzed in this study are publicly available: SGD phenotype annotations, GenAge model organisms (Build 21), CellAge (Build 3), Alliance of Genome Resources orthology (version 9.0.0), NCBI Gene (gene_info files), STRING (version 12.5), g:Profiler, Human Protein Atlas subcellular data, MGI phenotype and ortholog reports, and Gene Ontology (go-basic release 2026-07-26; UniProt-GOA human annotations of 11 October 2026). The harmonized catalog and all derived tables are provided in Supplementary Tables S1–S10.

Code availability Analysis scripts (12–22) and intermediate output tables are provided in the supplementary package.

Ethics approval Not applicable. This study analyzed only publicly available data and involved no human participants or animals.

Consent to participate and consent for publication Not applicable.

References

Alliance of Genome Resources Consortium (2024) Updates to the Alliance of Genome Resources central infrastructure. Genetics 227(1):iyae049. https://doi.org/10.1093/genetics/iyae049

Avelar RA, Ortega JG, Tacutu R et al (2020) A multidimensional systems biology analysis of cellular senescence in aging and disease. Genome Biol 21:91. https://doi.org/10.1186/s13059-020-01990-9

Baldarelli RM, Smith CL, Ringwald M et al (2024) Mouse Genome Informatics: an integrated knowledgebase system for the laboratory mouse. Genetics 227:iyae031. https://doi.org/10.1093/genetics/iyae031

Blondel VD, Guillaume JL, Lambiotte R, Lefebvre E (2008) Fast unfolding of communities in large networks. J Stat Mech 2008:P10008. https://doi.org/10.1088/1742-5468/2008/10/P10008

Budovsky A, Abramovich A, Cohen R, Chalifa-Caspi V, Fraifeld V (2007) Longevity network: construction and implications. Mech Ageing Dev 128:117–124. https://doi.org/10.1016/j.mad.2006.11.018

Coppé JP, Patil CK, Rodier F et al (2008) Senescence-associated secretory phenotypes reveal cell-nonautonomous functions of oncogenic RAS and the p53 tumor suppressor. PLoS Biol 6:2853–2868. https://doi.org/10.1371/journal.pbio.0060301

de Magalhães JP, Abidi Z, Dos Santos GA et al (2024) Human Ageing Genomic Resources: updates on key databases in ageing research. Nucleic Acids Res 52:D900–D908. https://doi.org/10.1093/nar/gkad927

Ellis HM, Horvitz HR (1986) Genetic control of programmed cell death in the nematode C. elegans. Cell 44:817–829. https://doi.org/10.1016/0092-8674(86)90004-8

Engel SR, Aleksander S, Nash RS et al (2025) Saccharomyces Genome Database: advances in genome annotation, expanded biochemical pathways, and other key enhancements. Genetics 229(3):iyae185. https://doi.org/10.1093/genetics/iyae185

Gene Ontology Consortium, Aleksander SA, Balhoff J et al (2023) The Gene Ontology knowledgebase in 2023. Genetics 224(1):iyad031. https://doi.org/10.1093/genetics/iyad031

Hamilton B, Dong Y, Shindo M et al (2005) A systematic RNAi screen for longevity genes in C. elegans. Genes Dev 19:1544–1555. https://doi.org/10.1101/gad.1308205

Hansen M, Hsu AL, Dillin A, Kenyon C (2005) New genes tied to endocrine, metabolic, and dietary regulation of lifespan from a Caenorhabditis elegans genomic RNAi screen. PLoS Genet 1:119–128. https://doi.org/10.1371/journal.pgen.0010017

Hayflick L, Moorhead PS (1961) The serial cultivation of human diploid cell strains. Exp Cell Res 25:585–621. https://doi.org/10.1016/0014-4827(61)90192-6

Herndon LA, Schmeissner PJ, Dudaronek JM et al (2002) Stochastic and genetic factors influence tissue-specific decline in ageing C. elegans. Nature 419:808–814. https://doi.org/10.1038/nature01135

Kaeberlein M, McVey M, Guarente L (1999) The SIR2/3/4 complex and SIR2 alone promote longevity in Saccharomyces cerevisiae by two different mechanisms. Genes Dev 13:2570–2580. https://doi.org/10.1101/gad.13.19.2570

Kenyon C, Chang J, Gensch E, Rudner A, Tabtiang R (1993) A C. elegans mutant that lives twice as long as wild type. Nature 366:461–464. https://doi.org/10.1038/366461a0

Kim J, Kundu M, Viollet B, Guan KL (2011) AMPK and mTOR regulate autophagy through direct phosphorylation of Ulk1. Nat Cell Biol 13:132–141. https://doi.org/10.1038/ncb2152

Kolberg L, Raudvere U, Kuzmin I et al (2023) g:Profiler — interoperable web service for functional enrichment analysis and gene identifier mapping (2023 update). Nucleic Acids Res 51:W207–W212. https://doi.org/10.1093/nar/gkad347

McCormick MA, Delaney JR, Tsuchiya M et al (2015) A comprehensive analysis of replicative lifespan in 4,698 single-gene deletion strains uncovers conserved mechanisms of aging. Cell Metab 22:895–906. https://doi.org/10.1016/j.cmet.2015.09.008

Mizushima N, Komatsu M (2011) Autophagy: renovation of cells and tissues. Cell 147:728–741. https://doi.org/10.1016/j.cell.2011.10.026

Mortimer RK, Johnston JR (1959) Life span of individual yeast cells. Nature 183:1751–1752. https://doi.org/10.1038/1831751a0

Rea SL, Wu D, Cypser JR, Vaupel JW, Johnson TE (2005) A stress-sensitive reporter predicts longevity in isogenic populations of Caenorhabditis elegans. Nat Genet 37:894–898. https://doi.org/10.1038/ng1608

Sancak Y, Peterson TR, Shaul YD et al (2008) The Rag GTPases bind raptor and mediate amino acid signaling to mTORC1. Science 320:1496–1501. https://doi.org/10.1126/science.1157535

Selman C, Tullet JMA, Wieser D et al (2009) Ribosomal protein S6 kinase 1 signaling regulates mammalian life span. Science 326:140–144. https://doi.org/10.1126/science.1177221

Serrano M, Lin AW, McCurrach ME, Beach D, Lowe SW (1997) Oncogenic ras provokes premature cell senescence associated with accumulation of p53 and p16INK4a. Cell 88:593–602. https://doi.org/10.1016/s0092-8674(00)81902-9

Sinclair DA, Guarente L (1997) Extrachromosomal rDNA circles — a cause of aging in yeast. Cell 91:1033–1042. https://doi.org/10.1016/s0092-8674(00)80493-6

Smith DL Jr, Maharrey CH, Carey CR, White RA, Hartman JL 4th (2016) Gene-nutrient interaction markedly influences yeast chronological lifespan. Exp Gerontol 86:113–123. https://doi.org/10.1016/j.exger.2016.04.012

Smith ED, Tsuchiya M, Fox LA et al (2008) Quantitative evidence for conserved longevity pathways between divergent eukaryotic species. Genome Res 18:564–570. https://doi.org/10.1101/gr.074724.107

Szklarczyk D, Nastou K, Koutrouli M et al (2025) The STRING database in 2025: protein networks with directionality of regulation. Nucleic Acids Res 53:D730–D737. https://doi.org/10.1093/nar/gkae1113

Tacutu R, Thornton D, Johnson E et al (2018) Human Ageing Genomic Resources: new and updated databases. Nucleic Acids Res 46:D1083–D1090. https://doi.org/10.1093/nar/gkx1042

Tsukada M, Ohsumi Y (1993) Isolation and characterization of autophagy-defective mutants of Saccharomyces cerevisiae. FEBS Lett 333:169–174. https://doi.org/10.1016/0014-5793(93)80398-e

Uhlén M, Fagerberg L, Hallström BM et al (2015) Tissue-based map of the human proteome. Science 347:1260419. https://doi.org/10.1126/science.1260419

Yanai H, Budovsky A, Barzilay T, Tacutu R, Fraifeld VE (2017) Wide-scale comparative analysis of longevity genes and interventions. Aging Cell 16:1267–1275. https://doi.org/10.1111/acel.12659

Yuan J, Shaham S, Ledoux S, Ellis HM, Horvitz HR (1993) The C. elegans cell death gene ced-3 encodes a protein similar to mammalian interleukin-1β-converting enzyme. Cell 75:641–652. https://doi.org/10.1016/0092-8674(93)90485-9

Supplementary Information

The supplementary package (Excel workbook, CSV files, scripts and figure files) contains:

- **Table S1.** All 116 core genes: direction in each organism, consensus, agreement, functional categories, STRING module and degree.
- **Table S2.** Functional enrichment of the core genes (g:Profiler) against the whole genome and against all aging-associated genes.
- **Table S3.** Convergence of genome-wide yeast deletion screens with each animal and human-cell dataset.
- **Table S4.** Subcellular location and developmental lethality by evidence group.
- **Table S5.** Logistic regression of developmental lethality adjusted for study intensity.
- **Table S6.** Developmental lethality of aging-promoting vs aging-restraining genes, overall and by system.
- **Table S7.** Full catalog of controlled genetic perturbations with human orthologs.
- **Table S8.** Permutation test for multi-organism genes; pairwise convergence with Benjamini–Hochberg q-values; functional categories; module summaries and stability; STRING edges; autophagy-core directions.
- **Table S9.** Predictions: 180 human genes with concordant effects in at least two non-mammalian organisms, a mouse ortholog and no controlled mouse lifespan data.

- **Table S10.** Directional-conservation tests: yeast RLS vs CLS, replication back-tests and human-cell vs organismal concordance by functional category.

Supplementary Files

This is a list of supplementary files associated with this preprint. Click to download.

- SupplementaryPackageBiogerontologyv5.zip
- SupplementaryTablesS1S10Biogerontology.xlsx